CORA Cork Open Research Archive
Cartlann Taighde Oscailte Chorcaí

Title	Modeling scattering matrix containing evanescent modes for wavefront shaping applications in disordered media
Authors	Raju, Michael;Jayet, Baptiste;Andersson-Engels, Stefan
Publication date	2026-07-29
Original Citation	Raju, M, Jayet, B & Andersson-Engels, S 2026, 'Modeling scattering matrix containing evanescent modes for wavefront shaping applications in disordered media', Physical Review Research, vol. 8, no. 3, 033123, pp. 1-16. https://doi.org/10.1103/86th-pl8q
Type of publication	Article (peer-reviewed)
Link to publisher's version	https://www.scopus.com/pages/publications/105046451268 - 10.1103/86th-pl8q
Rights	© 2026, the authors. Published by the American Physical Society under the terms of the Creative Commons Attribution 4.0 International license. Further distribution of this work must maintain attribution to the author(s) and the published article's title, journal citation, and DOI. - https://creativecommons.org/licenses/by/4.0/
Download date	2026-11-16 09:51:22
Item downloaded from	https://hdl.handle.net/10468/19199



University College Cork, Ireland
Coláiste na hOllscoile Corcaigh

Supplementary Material : Modeling scattering matrix containing evanescent modes for wavefront shaping applications in disordered media

Michael Raju,[1,2,*] Baptiste Jayet,[1] and Stefan Andersson-Engels[1,2]

[1] *Tyndall National Institute, Lee Maltings Complex, Dyke Parade, Cork, Ireland, T12 R5CP*
[2] *School of Physics, University College Cork, College Road, Cork, Ireland, T12 K8AF*

I. SPATIALLY CORRELATED DISORDERS

If the random disorder ensemble (characterized by its spatial refractive index fluctuations) drawn from a particular probability distribution is considered as a spatial random process, then according to the Wiener–Khinchin theorem, the randomness power spectrum of the disorder can be estimated by the spatial Fourier transform of its correlation function. Therefore, to create a random disorder with a particular correlation length, either the spatial correlation function (in real space) or the randomness power spectrum (in the spatial Fourier space) could be used. Here, we use the Fourier space method (as described in the Supplementary Sec. I A), for generating a uniformly-distributed Gaussian-correlated disorder. The disorder is represented in terms of the spatial dielectric-constant perturbation $\delta\tilde{\epsilon_r}(z,y)$ defined such that it is uniformly distributed with zero-mean and has a Gaussian spatial correlation. To characterize the disorder, variance is defined as $var_{disorder} = \langle\delta\tilde{\epsilon_r}(r)^2\rangle - \langle\delta\tilde{\epsilon_r}(r)\rangle^2 = \langle\delta\tilde{\epsilon_r}(r)^2\rangle$. The spatial correlation function can be defined as $R(k_{ref}r, k_{ref}r_0) = \langle\delta\tilde{\epsilon_r}(k_{ref}z, k_{ref}y)\delta\tilde{\epsilon_r}(k_{ref}z_0, k_{ref}y_0)\rangle$, where $R(k_{ref}r, k_{ref}r_0)$ is the un-normalized spatial correlation function. For a statistically homogeneous disorder, $R(k_{ref}r, k_{ref}r_0) = R(k_{ref}|r - r_0|)$. It can be noted from the definition of the disorder variance that $R(k_{ref}r_0, k_{ref}r_0) = R(0) = var_{disorder}$. Therefore, to represent the un-normalized spatial correlation function of the disorder, $R(0)$ value can be combined with a normalized correlation function $C_{disorder}(k_{ref}|r - r_0|)$ as given below

$$R(k_{ref}|r - r_0|) = R(0)C_{disorder}(k_{ref}|r - r_0|), \tag{1}$$

where the normalized two-point Gaussian spatial correlation function, $C_{disorder}(k_{ref}|r-r_0|)$ for $\delta\tilde{\epsilon_r}(r)$ as the following

$$C_{disorder}(k_{ref}|r - r_0|) = e^{-(k_{ref}|r-r_0|)^2/(k_{ref}^2 l_c^2)} \tag{2}$$

The power spectral density of the disorder ($P_{PSD}(p_z, p_y)$) is defined as the Fourier transform ($\mathcal{F}$) of the spatial correlation function.

$$P_{PSD}(p_z, p_y) = \mathcal{F}\{R(k_{ref}|r - r_0|)\} = var_{disorder}\mathcal{F}\{C_{disorder}(r, l_c)\} \tag{3}$$

where p_z and p_y are angular spatial frequencies. Having reviewed the essential concepts, using the numerical algorithm given in supplementary Sec. I A, a uniformly distributed-spatially correlated disorder is modeled.

A. Method for generating uniformly-distributed spatially-correlated disorder

The steps for estimating the uniformly-distributed Gaussian-correlated disorder are given as the following.

1. Estimate $\delta\epsilon_{\texttt{fft}}^{white} = \texttt{fft2}(\delta\epsilon_r^{white}(z,y))$ where `fft2` is the two dimensional Fourier transform and $\delta\epsilon_r^{white}(z,y)$ is the white-noise like uncorrelated disorder generated from a uniform probability distribution.
2. Take an element-wise product in the Fourier space to obtain $\delta\epsilon_{\texttt{fft}}^{corr} = \delta\epsilon_{\texttt{fft}}^{white}\mathcal{F}\{C_{disorder}(r, l_c)\}$
3. Apply inverse Fourier transform to estimate the correlated disorder in the real space with spatial correlation length l_c, given by $\delta\epsilon_r^{corr}(z,y) = \texttt{ifft2}(\delta\epsilon_{\texttt{fft}}^{corr})$ where `ifft2` is the two dimensional inverse Fourier transform.
4. Normalize $\delta\epsilon_r^{corr}(z,y)$ by dividing it with the standard deviation of the matrix elements. This results in a Gaussian distributed (with unit variance) and Gaussian correlated (with correlation length l_c) disorder.

* michaelraju@umail.ucc.ie

5. To transform the Gaussian distributed-Gaussian correlated disorder to a uniform distributed-Gaussian correlated disorder, a Gaussian cumulative probability distribution function ($C.D.F$) can be used. A zero mean Gaussian $C.D.F$ takes a normally distributed random variable and converts it into a transformed random variable between $(0,1)$ giving a uniform distribution. Hence, every matrix element of Gaussian distributed-Gaussian correlated disorder can be transformed between $(0,1)$ using the Gaussian $C.D.F$. Such a uniformly distributed disorder between $(0,1)$ can then be scaled between $min\left\{\delta\epsilon^{white}\right\}$ and $max\left\{\delta\epsilon^{white}\right\}$ to have similar spread in values with that of the uncorrelated white-noise like disorder.

6. Real space spatial correlation of the obtained disorder can be numerically estimated and validated against the l_c value used for defining the correlation function by the following method. It involves the Fourier space method for evaluating spatial autocorrelation of a $2D$ matrix. For an $M \times N$ correlated disorder $\delta\epsilon_r^{corr}(z,y)$,

$$R_{disorder}(k_{ref}|r-r_0|) = |\texttt{ifft2}\left[\texttt{fft2}(\delta\epsilon_r^{corr})(\texttt{fft2}(\delta\epsilon_r^{corr}))^*\right]|/(\texttt{MN}) \tag{4}$$

where $*$ denotes complex conjugation. Numerically estimated correlation length can be defined as the length at which the correlation function decays from $R(0)$ to $R(0)/e$.

II. NUMERICAL DISCRETIZATION SCHEME IMPLEMENTED

To represent the analytical functions presented in this paper as functions of z and y in numerical computations, we use numerical grids from the finite difference methods. These numerical grids have a finite grid cell size, Δ_z and Δ_y. For the analytical expressions given in the paper to be exact on the grid, Δ_z and Δ_y would need to tend to zero, which is practically infeasible due to the memory and computational processing limitations. Therefore, Δ_z and Δ_y are chosen as a trade-off (to be explained later) such that they are small enough to resolve wave states on the grids (especially evanescent eigenmodes), but not so small as to exhaust available memory and the processing capacity. Let there be N_z grid points/nodes along the z direction and N_y along the y direction so that the total number of grid points is N_zN_y, with the grid spacing Δ_z and Δ_y. The longitudinal size of the region is then $(N_z-1)\Delta_z$, and transverse size is $(N_y-1)\Delta_y$. Let the indices be $z_i = [1,2,...,N_z]$ and $y_j = [1,2,...,N_y]$. Then, the discrete values of z and y are given by $z = (z_i-1)\Delta_z$ and $y = (y_j-1)\Delta_y$, respectively, which form an array of values for z and y. Additionally, we define $W = (N_y-1)\Delta_y$. The analytical form of the propagating eigenmode, $\psi^{\pm}_{m,pr}(z,y) = \frac{1}{\sqrt{k_z^{(m)}}}e^{\pm ik_z^{(m)}z}\chi_m(y)$, needs to be discretized as follows. Let the discrete version of $\psi^{+}_{m,pr}(z_i,y_j)$ on the finite difference grid be written as

$$\psi^{+}_{m,pr}(z_i,y_j) = \underbrace{c_m^+ e^{+ik_z^{(m)}\Delta_z(z_i-1)}}_{\Phi^+_{m,pr}(z_i)}\chi_m(y_j) \tag{5}$$

where the coefficient c_m^+ is determined next, using the fact that the wave current injected by all normalized eigenmodes are unity. Here,

$$\chi_m(y_j) = \sqrt{\frac{2}{W}}\sin\{k_y^{(m)}\Delta_y(y_j-1)\} \tag{6}$$

with the discrete form of orthogonality relationship given by

$$\sum_{y_j}\chi_m(y_j)\chi_n(y_j)\Delta_y = \delta_{kron}(m,n) \tag{7}$$

The magnitude of the Z component of the flux density of the m^{th} eigenmode is defined as $J_z^{(m)}(z,y) = \mathfrak{Im}\left\{\psi_m^*(z,y)\frac{\partial}{\partial z}\psi_m(z,y)\right\}$, where $\mathfrak{Im}$ refers to the imaginary part. Using the centered first-order finite difference formula,

$$\frac{d}{dz}\Phi^+_{m,pr}(z_i) = \frac{\Phi^+_{m,pr}(z_i+1)-\Phi^+_{m,pr}(z_i-1)}{2\Delta_z}, \tag{8}$$

the discrete version of the flux density along Z can be evaluated as

$$J_z^{(m)}(z_i,y_j) = \frac{\chi_m(y_j)^2}{2i}\{\Phi^+_{m,pr}(z_i)^*\frac{d}{dz}\Phi^+_{m,pr}(z_i) - \Phi^+_{m,pr}(z_i)\frac{d}{dz}\Phi^+_{m,pr}(z_i)^*\} \tag{9}$$

which, upon simplification yields,

$$J_z^{(m)}(z_i, y_j) = \frac{\chi_m(y_j)^2}{2i} \left\{ 2i \; {c_m^+}^2 \left(\frac{sin(k_z^{(m)}\Delta_z)}{\Delta_z} \right) \right\} \tag{10}$$

Next, we numerically enforce the wave current (or flux) injected by the propagating eigenmode to be unity. Integrating the $J_z^{(m)}(z_i, y_j)$ along Y (using discrete summation) to get the total flux and equating to unity,

$$\begin{aligned} &\sum_{y_j} J_z^{(m)}(z_i, y_j) \cdot \Delta_y = 1 \implies \sum_{y_j} \chi_m(y_j)^2 \Delta_y {c_m^+}^2 \left(\frac{sin(k_z^m \Delta_z)}{\Delta_z} \right) = 1 \implies \\ &{c_m^+}^2 \left(\frac{sin(k_z^{(m)}\Delta_z)}{\Delta_z} \right) \underbrace{\sum_{y_j} \chi_m(y_j)^2 \Delta_y}_{=1} = 1 \implies c_m^+ = \frac{1}{\sqrt{\frac{sin(k_z^{(m)}\Delta_z)}{\Delta_z}}} \end{aligned} \tag{11}$$

Substituting for c_m^+ into $\psi_m^+(z_i, y_j)$, the discrete form of eigenmode is obtained as

$$\psi_{m,pr}^{\pm}(z_i, y_j) = \overbrace{\frac{1}{\sqrt{\frac{\sin\left(k_z^{(m)}\Delta_z\right)}{\Delta_z}}} e^{\pm i k_z^{(m)} \Delta_z (z_i - 1)}}^{\Phi_m^{\pm}(z_i)} \chi_m(y_j) \tag{12}$$

This discrete form of eigenmodes ensures flux conservation upon discretization and approaches the continuous analytic form $\psi_{m,pr}^{\pm}(z, y) = \frac{1}{\sqrt{k_z^{(m)}}} e^{\pm i k_z^{(m)} z} \chi_m(y)$, in the limit $\Delta_z \to 0$ and $\Delta_y \to 0$, since $lim_{\Delta_z \to 0} \frac{\sin\left(k_z^{(m)}\Delta_z\right)}{\Delta_z} = k_z^{(m)}$. In numerical implementation, the product $k_y^{(m)}\Delta_y$ is treated as a single term (dimensionless), to avoid precision errors when evaluating $\chi_m(y)$, since $k_y^{(m)}$ is significantly larger than Δ_y. Similarly, $k_z^{(m)}\Delta_z$ is also treated as a single variable.

For the evanescent modes where $k_z^{(m)} = i k_{z,ev}^{(m)}$, the analytical expression $\Phi_{m,ev}^{\pm}(z, z_{L/R}) = \frac{1}{\sqrt{|k_z^{(m)}|}} e^{-k_{z,ev}^{(m)} |z - z_{L/R}|}$ gets replaced by its discretized form given as

$$\Phi_{m,ev}^{\pm}(z_i, z_{i_{L/R}}) = \frac{1}{\sqrt{\frac{sin\left(|k_z^{(m)}|\Delta_z\right)}{\Delta_z}}} e^{-k_{z,ev}^{(m)} \Delta_z |z_i - z_{i_{L/R}}|} \tag{13}$$

Here, the subscript L/R denotes the left (L) or the right (R) boundary. Next, we discretize the continuous analytical dispersion relation $\left(\left(k_z^{(m)}\right)^2 + \left(k_y^{(m)}\right)^2 = k_{ref}^2 \right)$. By substituting the discrete form of eigenmodes in the discrete Helmholtz wave equation, the discrete dispersion relation is obtained as

$$\frac{4}{\Delta_z^2} sin^2 \left(\frac{k_z^{(m)}\Delta_z}{2} \right) + \frac{4}{\Delta_y^2} sin^2 \left(\frac{k_y^{(m)}\Delta_y}{2} \right) = k_{ref}^2 \tag{14}$$

Taking the limits, $lim_{\Delta_z \to 0}$ and $lim \Delta_y \to 0$, the continuous analytic dispersion relation is recovered.

For ease of implementation in numeric computations, we set $\Delta_z = \Delta_y = \Delta$ and Δ is chosen such that it adequately resolves the evanescent eigenmode with the highest transverse spatial frequency, $k_{y,max}^{(m)} = M_{total}\pi/W$ where $M_{total} = M_{pr} + M_{ev}$ is the total number of eigenmodes considered. The discretization resolution is chosen such that $k_{y,max}^{(m)}\Delta = 1$.

Similar to that of eigenmodes, the unperturbed Green's function is also discretized for numerical implementation as follows :

$$\begin{aligned} &G_0(z_i, y_j, z_{0i}, y_{0j}) = \\ &\sum_{m=1}^{\infty} d_m e^{i k_z^{(m)} |\Delta_z (z_i - z_{0_i})|} \sqrt{\frac{2}{W}} sin\left(k_y^{(m)} \Delta_y (y_j - 1) \right) \sqrt{\frac{2}{W}} sin\left(k_y^{(m)} (y_{0_j} - 1) \right) \end{aligned} \tag{15}$$

where,

$$d_m = \begin{cases} \frac{1}{2i\left(\frac{\sin(k_z^m \Delta_z)}{\Delta_z}\right)}, & \text{for propagating modes, } m \leq M_{pr} \\ \frac{1}{-2\left(\frac{\sin(|k_z^m| \Delta_z)}{\Delta_z}\right)}, & \text{for evanescent modes, } m > M_{pr} \end{cases} \tag{16}$$

III. ESTIMATING THE PERTURBED GREEN'S FUNCTION $G(r, r_0)$

The discretized Dyson's equation in $2D$ is $G_{ij} = G_{ij}^{(0)} + \sum_{k=1}^{k=N_z^P N_y^P} G_{ik}^{(0)} V_k \Delta_{area} G_{kj}$ where k is used as a index. The entire computational domain which includes the disordered perturbation region and the surrounding region for field visualization, has the size of $[N_y \times N_z]$. The disorder perturbation region has the size of $[N_y^P \times N_z^P]$, which is a subset of the computational domain $[N_y \times N_z]$. Therefore, there are $N_z^P N_y^P$ scatterer perturbation points. Here, the index i denotes the field evaluation location accessed linearly as a $1D$ array. Similarly, the index j denotes the source location accessed linearly as a $1D$ array, placed on the boundaries Γ_L or Γ_R. The index k accessed linearly as a $1D$ array, is associated with the locations at which the scatterer perturbation exists. Two methods are presented as the following where the first method is the direct matrix inversion method. Such a method is easier to understand, but it is memory intensive. The second method is the iterative method which requires iteration steps, but it is memory efficient.

Both the methods start by estimating the free space Green's function $G_{ik}^{(0)}$ and $G_{ij}^{(0)}$, where i spans all the field evaluation points of size $N_y N_z$ for visualisation purposes, k spans all the $N_z^P N_y^P$ scatterer position points where the perturbation is about to be brought in, and j the N_y points associated with the left or the right boundary. $G_{ik}^{(0)}$ is of the dimension $\left[N_y N_z \times N_y^P N_z^P\right]$. Other Green's function terms to be appearing in the methods can be derived as a subset from $G_{ik}^{(0)}$ and $G_{ij}^{(0)}$.

A. Direct method

Step 1 : Using the Dyson's equation, solve for G_{kj} for different locations of $k = k_1, k_2, k_3, ..., k_{N_z^P N_y^P}$ and a given j location

$$G_{k_1 j} = G_{k_1 j}^{(0)} + \begin{bmatrix} G_{k_1 k_1}^{(0)} V_{k_1} & G_{k_1 k_2}^{(0)} V_{k_2} & ... & G_{k_1 k_{N_y^P N_z^P}}^{(0)} V_{k_{N_z^P N_y^P}} \end{bmatrix} \begin{pmatrix} \Delta_{area} G_{k_1 j} \\ \Delta_{area} G_{k_2 j} \\ ... \\ \Delta_{area} G_{k_{(N_y^P N_z^P)} j} \end{pmatrix} \tag{17}$$

$$G_{k_2 j} = G_{k_2 j}^{(0)} + \begin{bmatrix} G_{k_2 k_1}^{(0)} V_{k_1} & G_{k_2 k_2}^{(0)} V_{k_2} & ... & G_{k_2 k_{N_y^P N_z^P}}^{(0)} V_{k_{N_z^P N_y^P}} \end{bmatrix} \begin{pmatrix} \Delta_{area} G_{k_1 j} \\ \Delta_{area} G_{k_2 j} \\ ... \\ \Delta_{area} G_{k_{(N_y^P N_z^P)} j} \end{pmatrix} \tag{18}$$

$$\vdots$$

$$G_{k_{(N_z^P N_y^P)} j} = G_{k_{(N_z^P N_y^P)} j}^{(0)} + \begin{bmatrix} G_{k_{(N_z^P N_y^P)} k_1}^{(0)} V_{k_1} & G_{k_{(N_z^P N_y^P)} k_2}^{(0)} V_{k_2} ... & G_{k_{(N_z^P N_y^P)} k_{N_y^P N_z^P}}^{(0)} V_{k_{N_z^P N_y^P}} \end{bmatrix} \begin{pmatrix} \Delta_{area} G_{k_1 j} \\ \Delta_{area} G_{k_2 j} \\ ... \\ \Delta_{area} G_{k_{(N_y^P N_z^P)} j} \end{pmatrix} \tag{19}$$

These set of equations can be written in a matrix form as

$$\begin{pmatrix} G_{k_1 j} \\ G_{k_2 j} \\ G_{k_3 j} \\ \vdots \\ G_{k_{(N_z^P N_y^P)} j} \end{pmatrix} = \begin{pmatrix} G^{(0)}_{k_1 j} \\ G^{(0)}_{k_2 j} \\ G^{(0)}_{k_3 j} \\ \vdots \\ G^{(0)}_{k_{(N_z^P N_y^P)} j} \end{pmatrix} + \underbrace{\begin{pmatrix} G^{(0)}_{k_1 k_1} V_{k_1} & G^{(0)}_{k_1 k_2} V_{k_2} & \dots & G^{(0)}_{k_1 k_{(N_z^P N_y^P)}} V_{k_{(N_z^P N_y^P)}} \\ G^{(0)}_{k_2 k_1} V_{k_1} & G^{(0)}_{k_2 k_2} V_{k_2} & \dots & G^{(0)}_{k_2 k_{(N_z^P N_y^P)}} V_{k_{(N_z^P N_y^P)}} \\ G^{(0)}_{k_3 k_1} V_{k_1} & G^{(0)}_{k_3 k_2} V_{k_2} & \dots & G^{(0)}_{k_3 k_{(N_z^P N_y^P)}} V_{k_{(N_z^P N_y^P)}} \\ \vdots & \vdots & \vdots & \vdots \\ G^{(0)}_{k_{(N_z^P N_y^P)} k_1} V_{k_1} & G^{(0)}_{k_{(N_z^P N_y^P)} k_2} V_{k_2} & \dots & G^{(0)}_{k_{(N_z^P N_y^P)} k_{(N_z^P N_y^P)}} V_{k_{(N_z^P N_y^P)}} \end{pmatrix}}_{M} \begin{pmatrix} \Delta_{area} G_{k_1 j} \\ \Delta_{area} G_{k_2 j} \\ \Delta_{area} G_{k_3 j} \\ \vdots \\ \Delta_{area} G_{k_{(N_z^P N_y^P)} j} \end{pmatrix} \tag{20}$$

Representing the same system of equations as a matrix equation, G_{kj} is solved involving an M matrix (M matrix defined in the above given equation), as given below

$$\begin{aligned} [G_{kj}] &= \left[G^{(0)}_{kj}\right] + [M]\,[G_{kj}] \implies \\ [G_{kj}] &= [I - [M]]^{-1} \left[G^{(0)}_{kj}\right] \end{aligned} \tag{21}$$

Step 2 : Once $[G_{kj}]$ is obtained, evaluate $[G_{ij}]$ for a given j

$$\begin{pmatrix} G_{i_1 j} \\ G_{i_2 j} \\ G_{i_3 j} \\ \vdots \\ G_{i_{(N_z N_y)} j} \end{pmatrix} = \begin{pmatrix} G^{(0)}_{i_1 j} \\ G^{(0)}_{i_2 j} \\ G^{(0)}_{i_3 j} \\ \vdots \\ G^{(0)}_{i_{(N_z N_y)} j} \end{pmatrix} + \begin{pmatrix} G^{(0)}_{i_1 k_1} V_{k_1} & G^{(0)}_{i_1 k_2} V_{k_2} & \dots & G^{(0)}_{i_1 k_{(N_z^P N_y^P)}} V_{k_{(N_z^P N_y^P)}} \\ G^{(0)}_{i_2 k_1} V_{k_1} & G^{(0)}_{i_2 k_2} V_{k_2} & \dots & G^{(0)}_{i_2 k_{(N_z^P N_y^P)}} V_{k_{(N_z^P N_y^P)}} \\ G^{(0)}_{i_3 k_1} V_{k_1} & G^{(0)}_{i_3 k_2} V_{k_2} & \dots & G^{(0)}_{i_3 k_{(N_z^P N_y^P)}} V_{k_{(N_z^P N_y^P)}} \\ \vdots & \vdots & \vdots & \vdots \\ G^{(0)}_{i_{(N_z N_y)} k_1} V_{k_1} & G^{(0)}_{i_{(N_z N_y)} k_2} V_{k_2} & \dots & G^{(0)}_{i_{(N_z N_y)} k_{(N_z^P N_y^P)}} V_{k_{(N_z^P N_y^P)}} \end{pmatrix} \begin{pmatrix} \Delta_{area} G_{k_1 j} \\ \Delta_{area} G_{k_2 j} \\ \Delta_{area} G_{k_3 j} \\ \vdots \\ \Delta_{area} G_{k_{(N_z^P N_y^P)} j} \end{pmatrix} \tag{22}$$

where there is $N_z N_y$ field evaluation points due to $N_z^P N_y^P$ scattering particles. With step 1 and step 2 evaluated for different source locations j, G_{ij} can be fully solved. Although the direct method presented in this subsection is short and easy to understand, it is memory intensive because of the formation of the large non-sparse M matrix (of size $N_z^P N_y^P \times N_z^P N_y^P$) and the associated inversion process in the Eq. 21. Also, the free space Green's function $G^{(0)}_{ik}$ needs to be evaluated for the i corresponding to the entire $[N_z \times N_y]$ grid for the purpose of visualization. The location k needs to be spanned through all the scattering particle locations (to evaluate the M matrix), consuming memory. To save memory the following iterative method is used instead.

B. Iterative method involving slices of scatterers

In the iterative method, the total scattering block is divided into slices and the Green's function is updated accounting the scattering effect of the slices taken one at a time. As an example, let's say the entire scattering region

is divided into 10 slices. $G^{(0)}_{ik}$ needs to be evaluated like before for the source k location spanning all the particle positions. $G^{(0)}_{ij}$ is also evaluated where j is on Γ_L or Γ_R. Accounting the scattering perturbation of slice number 1 yields the new updated Green's function $G^{(1)}_{ik}$. While evaluating $G^{(1)}_{ik}$, the source k locations needs to be only those scatterer positions where the remaining 9 slices are to be brought in and also on the boundaries. One could overwrite the $G^{(0)}_{ik}$ array data (only for the source locations of the particles to be brought in, corresponding to the remaining 9 slices) for saving memory. Now the second slice is brought in and $G^{(1)}_{ik}$ is used to evaluate $G^{(2)}_{ik}$ accounting the scattering effect of the second slice. For evaluating $G^{(2)}_{ik}$, the source k locations needs to be only those scatterer locations where the remaining 8 slices are to be brought in and also on the boundaries. The method is repeated by bringing in the remaining slices one by one and updating the Green's function by overwriting the previous version, for the remaining particle positions. Therefore, the process becomes faster upon progressing through the slices.

First, let the first transverse slice of the scatterers be chosen, numbered $1 : N^P_y$ denoted as $1 \rightarrow N^P_y$. Solve the Eq. 20 just for the first slice.

Main step 1 for the iteration method involving the first slice of scatterers

- *Sub-step 1:*

$$\begin{pmatrix} G^{(1)}_{k_1 j} \\ G^{(1)}_{k_2 j} \\ G^{(1)}_{k_3 j} \\ \vdots \\ G^{(1)}_{k_{(N^P_y)} j} \end{pmatrix} = \begin{pmatrix} G^{(0)}_{k_1 j} \\ G^{(0)}_{k_2 j} \\ G^{(0)}_{k_3 j} \\ \vdots \\ G^{(0)}_{k_{(N^P_y)} j} \end{pmatrix} + \underbrace{\begin{pmatrix} G^{(0)}_{k_1 k_1} V_{k_1} & G^{(0)}_{k_1 k_2} V_{k_2} & \dots & G^{(0)}_{k_1 k_{(N^P_y)}} V_{k_{(N^P_y)}} \\ G^{(0)}_{k_2 k_1} V_{k_1} & G^{(0)}_{k_2 k_2} V_{k_2} & \dots & G^{(0)}_{k_2 k_{(N^P_y)}} V_{k_{(N^P_y)}} \\ G^{(0)}_{k_3 k_1} V_{k_1} & G^{(0)}_{k_3 k_2} V_{k_2} & \dots & G^{(0)}_{k_3 k_{(N^P_y)}} V_{k_{(N^P_y)}} \\ \vdots & \vdots & \vdots & \vdots \\ G^{(0)}_{k_{(N^P_y)} k_1} V_{k_1} & G^{(0)}_{k_{(N^P_y)} k_2} V_{k_2} & \dots & G^{(0)}_{k_{(N^P_y)} k_{(N^P_y)}} V_{k_{(N^P_y)}} \end{pmatrix}}_{M^{(0)}_{(1 \rightarrow N^P_y)}} \begin{pmatrix} \Delta_{area} G^{(1)}_{k_1 j} \\ \Delta_{area} G^{(1)}_{k_2 j} \\ \Delta_{area} G^{(1)}_{k_3 j} \\ \vdots \\ \Delta_{area} G^{(1)}_{k_{(N^P_y)} j} \end{pmatrix} \tag{23}$$

- *Sub-step 2:* Representing the above given system of equations as a matrix equation, $G^{(1)}_{k_{(1 \rightarrow N^p_y)} j}$ is solved involving the $M^{(0)}_{(1 \rightarrow N^P_y)}$ matrix (defined in the previous equation), as given below

$$\begin{aligned} \left[G^{(1)}_{k_{(1 \rightarrow N^p_y)} j} \right] &= \left[G^{(0)}_{k_{(1 \rightarrow N^p_y)} j} \right] + \left[M^{(0)}_{(1 \rightarrow N^P_y)} \right] \left[G^{(1)}_{k_{(1 \rightarrow N^p_y)} j} \right] \implies \\ \left[G^{(1)}_{k_{(1 \rightarrow N^p_y)} j} \right] &= \left[I - \left[M^{(0)}_{(1 \rightarrow N^P_y)} \right] \right]^{-1} \left[G^{(0)}_{k_{(1 \rightarrow N^p_y)} j} \right] \end{aligned} \tag{24}$$

- *Sub-step 3:* Once $[G^{(1)}_{k_{(1 \rightarrow N^p_y)} j}]$ is obtained, evaluate $[G^{(1)}_{ij}]$ for a given j

$$\begin{pmatrix} G^{(1)}_{i_1 j} \\ G^{(1)}_{i_2 j} \\ G^{(1)}_{i_3 j} \\ \vdots \\ G^{(1)}_{i_{(N_z N_y)} j} \end{pmatrix} = \begin{pmatrix} G^{(0)}_{i_1 j} \\ G^{(0)}_{i_2 j} \\ G^{(0)}_{i_3 j} \\ \vdots \\ G^{(0)}_{i_{(N_z N_y)} j} \end{pmatrix} + \begin{pmatrix} G^{(0)}_{i_1 k_1} V_{k_1} & G^{(0)}_{i_1 k_2} V_{k_2} & \dots & G^{(0)}_{i_1 k_{(N^P_y)}} V_{k_{(N^P_y)}} \\ G^{(0)}_{i_2 k_1} V_{k_1} & G^{(0)}_{i_2 k_2} V_{k_2} & \dots & G^{(0)}_{i_2 k_{(N^P_y)}} V_{k_{(N^P_y)}} \\ G^{(0)}_{i_3 k_1} V_{k_1} & G^{(0)}_{i_3 k_2} V_{k_2} & \dots & G^{(0)}_{i_3 k_{(N^P_y)}} V_{k_{(N^P_y)}} \\ \vdots & \vdots & \vdots & \vdots \\ G^{(0)}_{i_{(N_z N_y)} k_1} V_{k_1} & G^{(0)}_{i_{(N_z N_y)} k_2} V_{k_2} & \dots & G^{(0)}_{i_{(N_z N_y)} k_{(N^P_y)}} V_{k_{(N^P_y)}} \end{pmatrix} \begin{pmatrix} \Delta_{area} G^{(1)}_{k_1 j} \\ \Delta_{area} G^{(1)}_{k_2 j} \\ \Delta_{area} G^{(1)}_{k_3 j} \\ \vdots \\ \Delta_{area} G^{(1)}_{k_{(N^P_y)} j} \end{pmatrix} \tag{25}$$

- *Sub-step 4:* Before moving onto the next main iteration step (main iteration step number 2), the following sub-step evaluations has to be performed to estimate $[G^{(1)}_{k_{(1 \rightarrow N^p_y)} k_{(N^p_y + 1 \rightarrow N^p_y N^p_z)}}]$ and $[G^{(1)}_{i k_{(N^p_y + 1 \rightarrow N^p_y N^p_z)}}]$ to be used in the next main iteration step. Here $(N^p_y + 1 \rightarrow N^p_y N^p_z)$ corresponds to the remaining scatter position where the perturbation is brought-in in the future iteration steps by introducing slice number 2,3,4 etc..

Using Eq. 24,

$$\left[G^{(1)}_{k_{(1 \rightarrow N^p_y)} k_{(N^p_y + 1 \rightarrow N^p_y N^p_z)}} \right] = \left[I - \left[M^{(0)}_{(1 \rightarrow N^P_y)} \right] \right]^{-1} \left[G^{(0)}_{k_{(1 \rightarrow N^p_y)} k_{(N^p_y + 1 \rightarrow N^p_y N^p_z)}} \right] \tag{26}$$

Taking Eq. 25 and substituting for j as $k_{(N_y^p+1\rightarrow N_y^p N_z^p)}$, together with the above given equation, $[G^{(1)}_{ik_{(N_y^p+1\rightarrow N_y^p N_z^p)}}]$ can be estimated. The estimated $[G^{(1)}_{ik_{(N_y^p+1\rightarrow N_y^p N_z^p)}}]$ can be overwritten upon the existing memory taken by $G^{(0)}_{ik}$.

Main step 2 involving the second slice of scatterers denoted by $N_y^P+1\rightarrow 2N_y^P$,

• *Sub-step 1:*

$$\begin{pmatrix} G^{(2)}_{k_{(N_y^P+1)}j} \\ G^{(2)}_{k_{(N_y^P+2)}j} \\ G^{(2)}_{k_{(N_y^P+3)}j} \\ \vdots \\ G^{(2)}_{k_{(2N_y^P)}j} \end{pmatrix} = \begin{pmatrix} G^{(1)}_{k_{(N_y^P+1)}j} \\ G^{(1)}_{k_{(N_y^P+2)}j} \\ G^{(1)}_{k_{(N_y^P+3)}j} \\ \vdots \\ G^{(1)}_{k_{(2N_y^P)}j} \end{pmatrix} +$$

$$\underbrace{\begin{pmatrix} G^{(1)}_{k_{(N_y^P+1)}k_{(N_y^P+1)}}V_{k_{(N_y^P+1)}} & G^{(1)}_{k_{(N_y^P+1)}k_{(N_y^P+2)}}V_{k_{(N_y^P+2)}} & \dots & G^{(1)}_{k_{(N_y^P+1)}k_{(2N_y^P)}}V_{k_{(2N_y^P)}} \\ G^{(1)}_{k_{(N_y^P+2)}k_{(N_y^P+1)}}V_{k_{(N_y^P+1)}} & G^{(1)}_{k_{(N_y^P+2)}k_{(N_y^P+2)}}V_{k_{(N_y^P+2)}} & \dots & G^{(1)}_{k_{(N_y^P+2)}k_{(2N_y^P)}}V_{k_{(2N_y^P)}} \\ G^{(1)}_{k_{(N_y^P+3)}k_{(N_y^P+1)}}V_{k_{(N_y^P+1)}} & G^{(1)}_{k_{(N_y^P+3)}k_{(N_y^P+2)}}V_{k_{(N_y^P+2)}} & \dots & G^{(1)}_{k_{(N_y^P+3)}k_{(2N_y^P)}}V_{k_{(2N_y^P)}} \\ \vdots & \vdots & \vdots & \vdots \\ G^{(1)}_{k_{(2N_y^P)}k_{(N_y^P+1)}}V_{k_{(N_y^P+1)}} & G^{(1)}_{k_{(2N_y^P)}k_{(N_y^P+2)}}V_{k_{(N_y^P+2)}} & \dots & G^{(1)}_{k_{(2N_y^P)}k_{(2N_y^P)}}V_{k_{(2N_y^P)}} \end{pmatrix}}_{M^{(1)}_{(N_y^P+1\rightarrow 2N_y^P)}} \begin{pmatrix} \Delta_{area}G^{(2)}_{k_{(N_y^P+1)}j} \\ \Delta_{area}G^{(2)}_{k_{(N_y^P+2)}j} \\ \Delta_{area}G^{(2)}_{k_{(N_y^P+3)}j} \\ \vdots \\ \Delta_{area}G^{(2)}_{k_{(2N_y^P)}j} \end{pmatrix} \tag{27}$$

• *Sub-step 2:* Representing the above given system of equations as a matrix equation, $G^{(2)}_{k_{(N_y^p+1\rightarrow 2N_y^p)}j}$ is solved involving the $M^{(1)}_{(N_y^p+1\rightarrow 2N_y^P)}$ matrix (defined in the previous equation), as given below

$$\begin{aligned} \left[G^{(2)}_{k_{(N_y^p+1\rightarrow 2N_y^p)}j}\right] &= \left[G^{(1)}_{k_{(N_y^p+1\rightarrow 2N_y^p)}j}\right] + \left[M^{(1)}_{(N_y^p+1\rightarrow 2N_y^P)}\right]\left[G^{(2)}_{k_{(N_y^p+1\rightarrow 2N_y^p)}j}\right] \Longrightarrow \\ \left[G^{(2)}_{k_{(N_y^p+1\rightarrow 2N_y^p)}j}\right] &= \left[I - \left[M^{(1)}_{(N_y^p+1\rightarrow 2N_y^P)}\right]\right]^{-1}\left[G^{(1)}_{k_{(N_y^p+1\rightarrow 2N_y^p)}j}\right] \end{aligned} \tag{28}$$

• *Sub-step 3:* Once $[G^{(2)}_{k_{(N_y^p+1\rightarrow 2N_y^p)}j}]$ is obtained, evaluate $[G^{(2)}_{ij}]$ for a given j.

$$\begin{pmatrix} G^{(2)}_{i_1 j} \\ G^{(2)}_{i_2 j} \\ G^{(2)}_{i_3 j} \\ \vdots \\ G^{(2)}_{i_{(N_z N_y)}j} \end{pmatrix} = \begin{pmatrix} G^{(1)}_{i_1 j} \\ G^{(1)}_{i_2 j} \\ G^{(1)}_{i_3 j} \\ \vdots \\ G^{(1)}_{i_{(N_z N_y)}j} \end{pmatrix} +$$

$$\begin{pmatrix} G^{(1)}_{i_1 k_{(N_y^p+1)}}V_{k_{(N_y^p+1)}} & G^{(1)}_{i_1 k_{(N_y^p+2)}}V_{k_{(N_y^p+2)}} & \dots & G^{(1)}_{i_1 k_{(2N_y^P)}}V_{k_{(2N_y^P)}} \\ G^{(1)}_{i_2 k_{(N_y^p+1)}}V_{k_{(N_y^p+1)}} & G^{(1)}_{i_2 k_{(N_y^p+2)}}V_{k_{(N_y^p+2)}} & \dots & G^{(1)}_{i_2 k_{(2N_y^P)}}V_{k_{(2N_y^P)}} \\ G^{(1)}_{i_3 k_{(N_y^p+1)}}V_{k_{(N_y^p+1)}} & G^{(1)}_{i_3 k_{(N_y^p+2)}}V_{k_{(N_y^p+2)}} & \dots & G^{(1)}_{i_3 k_{(2N_y^P)}}V_{k_{(2N_y^P)}} \\ \vdots & \vdots & \vdots & \vdots \\ G^{(1)}_{i_{(N_z N_y)}k_{(N_y^p+1)}}V_{k_{(N_y^p+1)}} & G^{(1)}_{i_{(N_z N_y)}k_{(N_y^p+2)}}V_{(k_{N_y^p+2})} & \dots & G^{(1)}_{i_{(N_z N_y)}k_{(2N_y^P)}}V_{k_{(2N_y^P)}} \end{pmatrix} \begin{pmatrix} \Delta_{area}G^{(2)}_{k_{(N_y^p+1)}j} \\ \Delta_{area}G^{(2)}_{k_{(N_y^p+2)}j} \\ \Delta_{area}G^{(2)}_{k_{(N_y^p+3)}j} \\ \vdots \\ \Delta_{area}G^{(2)}_{k_{(2N_y^P)}j} \end{pmatrix} \tag{29}$$

• *Sub-step 4:* Before moving onto the next main iteration step (main iteration step number 3), the following sub-step evaluations has to be performed to estimate $[G^{(2)}_{k_{(N_y^p+1\rightarrow 2N_y^p)}k_{(2N_y^p+1\rightarrow N_y^p N_z^p)}}]$ and $[G^{(2)}_{ik_{(2N_y^p+1\rightarrow N_y^p N_z^p)}}]$ to be used

in the next main iteration step. Here $(2N_y^p+1 \rightarrow N_y^p N_z^p)$ corresponds to the remaining scatter position where the perturbation is brought-in in the future iteration steps by introducing slice number 3,4,5 etc..

Using Eq. 28,

$$\left[G^{(2)}_{k_{(N_y^p+1\rightarrow 2N_y^p)}k_{(2N_y^p+1\rightarrow N_y^p N_z^p)}}\right] = \left[I - \left[M^{(1)}_{(N_y^p+1\rightarrow 2N_y^P)}\right]\right]^{-1}\left[G^{(1)}_{k_{(N_y^p+1\rightarrow 2N_y^p)}k_{(2N_y^p+1\rightarrow N_y^p N_z^p)}}\right] \tag{30}$$

Taking Eq. 29 and substituting for j as $k_{(2N_y^p+1\rightarrow N_y^p N_z^p)}$, together with the above given equation, $[G^{(2)}_{ik_{(2N_y^p+1\rightarrow N_y^p N_z^p)}}]$ can be estimated. The estimated $[G^{(2)}_{ik_{(2N_y^p+1\rightarrow N_y^p N_z^p)}}]$ can be overwritten upon the existing memory taken by $G^{(1)}_{ik}$. Following the same logic, the main step 3 involving the slice of scatterers denoted by $2N_y^P+1 \rightarrow 3N_y^P$ can be evaluated. The iteration process continues until the last slice of scatterers are brought in, obtaining the fully perturbed Green's function G_{ij} .

IV. HOMOGENEOUS BOUNDARY CONDITIONS SATISFIED BY THE GREEN'S FUNCTION AND THE EIGENMODES

$$G(r,r_0)|_{z<z_0,(z,y)\in\Gamma_L} = \sum_{m=1}^{\infty} G_m(z,y,z_0,y_0)|_{z<z_0,(z,y)\in\Gamma_L} = \sum_{m=1}^{\infty} \underbrace{g_m^-(z_0,y_0)\psi_m^-(z,y)|_{z<z_0,(z,y)\in\Gamma_L}}_{G_m(z,y,z_0,y_0)|_{z<z_0,(z,y)\in\Gamma_L}} \tag{31}$$

$$G(r,r_0)|_{z\geq z_0,(z,y)\in\Gamma_R} = \sum_{m=1}^{\infty} G_m(z,y,z_0,y_0)|_{z\geq z_0,(z,y)\in\Gamma_R} = \sum_{m=1}^{\infty} \underbrace{g_m^+(z_0,y_0)\psi_m^+(z,y)|_{z\geq z_0,(z,y)\in\Gamma_R}}_{G_m(z,y,z_0,y_0)|_{z\geq z_0,(z,y)\in\Gamma_R}} \tag{32}$$

Both the propagating and the evanescent eigenmodes satisfy the following homogeneous boundary condition at the boundaries Γ_L and Γ_R,

$$\frac{\partial}{\partial z}\psi_m^{\pm}(z,y) \mp ik_z^m\psi_m^{\pm}(z,y) = 0, \tag{33}$$

where in particular $k_z^{(m)} = ik_{z,ev}^{(m)}$ for the evanescent eigenmodes. As the disorder perturbation doesn't change the boundary conditions of eigenmodes associated with the outgoing Green's function waves, the following homogeneous boundary condition can be formed in terms of $G_m(z,y,z_0,y_0)$ similar to that of Eq. 33.

$$\left\{\frac{\partial}{\partial z}G_m(r,r_0) + ik_z^{(m)}G_m(r,r_0)\right\}|_{z<z_0,(z,y)\in\Gamma_L} = 0 \tag{34}$$

$$\left\{\frac{\partial}{\partial z}G_m(r,r_0) - ik_z^{(m)}G_m(r,r_0)\right\}|_{z\geq z_0,(z,y)\in\Gamma_R} = 0 \tag{35}$$

V. SIMPLIFYING KIRCHHOFF–HELMHOLTZ BOUNDARY INTEGRAL EQUATION

As there is no flux flowing out of the transverse boundaries Γ_U and Γ_D, the boundary integral equation Eq. 16 can be simplified as

$$\begin{aligned}&\int\left\{\tilde{E}(r)\frac{\partial}{\partial z}G\left(r,r_0\right)\hat{e}_z - G\left(r,r_0\right)\frac{\partial}{\partial z}\tilde{E}(r)\hat{e}_z\right\}|_{(z,y)\in\Gamma_L}\cdot(-\hat{e}_z)\,dy+\\ &\int\left[\tilde{E}(r)\frac{\partial}{\partial z}G\left(r,r_0\right)\hat{e}_z - G\left(r,r_0\right)\frac{\partial}{\partial z}\tilde{E}(z,y)\hat{e}_z\right]|_{(z,y)\in\Gamma_R}\cdot\hat{e}_z dy = \tilde{E}\left(z_0,y_0\right)|_{(z_0,y_0)\in\Omega}\end{aligned} \tag{36}$$

There is a minus sign associated with the $-\hat{e}_z dy$ on the first integral of the L.H.S in Eq. 36. This is due to the sign convention that the surface normal $\hat{n}$ points outwards on Γ_L which is in opposite direction to $\hat{e}_z \frac{\partial}{\partial z}$ terms. The boundary integral equation Eq. 36, can be further simplified as both $G(z,z,y,y_0)$ and the total field $\tilde{E}(z,y,z_0,y_0)|_{(z,y)\in\Gamma_L or (z,y)\in\Gamma_R}$ can be expanded in terms of eigenmodes $\psi_m^{\pm}(z,y)|_{(z,y)\in\Gamma_{L/R}}$ followed by the use of associated boundary conditions to be explained as the following. Let the wave incidence be from the left side of the disorder onto Γ_L. The total wave on Γ_L is the sum of incident wave modes and reflected wave modes. As the $E(z,y)$ in Eq. 36 is the total field, the first step to simplify is to provide explicit expression for $\tilde{E}(z,y)$ close to the boundary Γ_L and Γ_R followed by the use boundary conditions involving z derivatives of $\tilde{E}(z,y)$ and $G(z,y,z_0,y_0)$ to be explained in the following section. For $(z,y)\in\Gamma_L$,

$$\tilde{E}(z,y) = \tilde{E}^{inc}(z,y) + \tilde{E}^{refl}(z,y), \tag{37}$$

$$\text{where } \tilde{E}_{inc}(z,y)|_{(z,y)\in\Gamma_L} = \sum_{m=1}^{M_{total}} c_m^+ \chi_m(y)\phi_m^+(z) \tag{38}$$

$$\text{such that } \phi_m^+(z) = \begin{cases} \phi_{m,pr}^+(z) \text{ when } m \le M_{pr} \\ \phi_{m,ev}^+(z,z_L) \text{ when } m > M_{pr} \end{cases} \text{ and}$$

$$\tilde{E}_{refl}(z,y)|_{(z,y)\in\Gamma_L} = \sum_{n=1}^{N_{total}} r_n^- \chi_n(y)\phi_n^-(z) \text{such that } \phi_n^-(z) = \begin{cases} \phi_{n,pr}^-(z) \text{ when } n \le N_{pr} \\ \phi_{n,ev}^-(z,z_L) \text{ when } n > N_{pr} \end{cases} \tag{39}$$

$$\text{and } r_n^- = \sum_{m=1}^{M_{total}} S_{11}^{nm} c_m^+ \tag{40}$$

Here, r_n^- is the reflection coefficient. Substituting equations Eq. 38 and Eq. 39 in Eq. 37, and using the property of the Kronecker delta function, the following is obtained.

$$\tilde{E}(z,y)|_{(z,y)\in\Gamma_L} = \sum_{n=1}^{N_{total}}\sum_{m=1}^{M_{total}} c_m^+\phi_m^+(z)\chi_m(y)\delta_{kron}(n,m)|_{(z,y)\in\Gamma_L} + \sum_{n=1}^{N_{total}}\sum_{m=1}^{M_{total}} c_m^+ S_{11}^{nm}\chi_n(y)\phi_n^-(z)|_{(z,y)\in\Gamma_L} \tag{41}$$

Due to the Kronecker delta on the first term on the R.H.S of the above given equation, the index m can be replaced by n to obtain

$$\tilde{E}(z,y)|_{(z,y)\in\Gamma_L} = \sum_{n=1}^{N_{total}} \underbrace{\sum_{m=1}^{M_{total}} c_m^+ \left\{\phi_n^+(z)\chi_n(y)\delta_{kron}(n,m) + S_{11}^{nm}\chi_n(y)\phi_n^-(z)\right\}}_{\tilde{E}_n(z,y)|_{(z,y)\in\Gamma_L}} = \sum_{n=1}^{N_{total}} \tilde{E}_n(z,y)|_{(z,y)\in\Gamma_L} \tag{42}$$

Eq. 42 denotes that the total field on Γ_L can be written as a series summation involving $\tilde{E}_n(z,y)|_{(z,y)\in\Gamma_L}$ waves. Next, the boundary condition associated with $\tilde{E}_n(z,y)|_{(z,y)\in\Gamma_L}$ waves for simplifying the boundary integral equation is provided.

$$\tfrac{\partial}{\partial z}\tilde{E}_n(z,y)|_{(z,y)\in\Gamma_L} + ik_z^{(n)}\tilde{E}_n(z,y)|_{(z,y)\in\Gamma_L} = \begin{cases} 2ik_z^{(n)}\tilde{E}_n^{inc}(z,y)|_{(z,y)\in\Gamma_L}, & \text{if } 1 \le n \le M_{total} \\ 0, & \text{if } n > M_{total} \end{cases} \tag{43}$$

where $\tilde{E}_n^{inc}(z,y)|_{(z,y)\in\Gamma_L} = c_n^+\psi_n^+(z,y)|_{(z,y)\in\Gamma_L}$ is the n^{th} eigenmode term associated with the incident wave incident on the disorder from the left and $k_z^{(n)} = ik_{z,ev}^{(n)}$ for evanescent waves. Next is to evaluate the transmitted total field on Γ_R due to the wave incidence from the left side upon Γ_L and the associated boundary condition.

$$\tilde{E}(z,y)|_{(z,y)\in\Gamma_R} = \tilde{E}^{trans}(z,y)|_{(z,y)\in\Gamma_R} = \sum_{n=1}^{N_{total}} t_n^+\phi_n^+(z)\chi_n(y)|_{(z,y)\in\Gamma_R} \tag{44}$$

$$\text{such that } \phi_n^+(z) = \begin{cases} \phi_{n,pr}^+(z) \text{ when } n \le N_{pr} \\ \phi_{n,ev}^+(z,z_R) \text{ when } n > N_{pr} \end{cases}$$

where the field transmission coefficient term t_n^+ is related to the transmission matrix S_{21} by

$$t_n^+ = \sum_{m=1}^{M_{total}} S_{21}^{nm} c_m^+ \tag{45}$$

Therefore,

$$\tilde{E}(z,y)|_{(z,y)\in\Gamma_R} = \sum_{n=1}^{N_{total}} \underbrace{\left\{ \sum_{m=1}^{M_{total}} c_m^+ S_{21}^{nm} \right\} \phi_n^+(z)\chi_n(y)\,|_{(z,y)\in\Gamma_R}}_{\tilde{E}_n(z,y)|_{(z,y)\in\Gamma_R}} \tag{46}$$

$$= \sum_{n=1}^{N_{total}} \tilde{E}_n(z,y)|_{(z,y)\in\Gamma_R} \tag{47}$$

Similar to that of Eq. 43, one could form a boundary condition for $E_n(z,y)|_{(z,y)\in\Gamma_R}$ on the right boundary Γ_R as given below, to be used to simplify the boundary integral equation given in Eq. 36. This homogeneous boundary condition can be easily verified using equations Eq. 46 and Eq. 47.

$$\frac{\partial}{\partial z}\tilde{E}_n(z,y)|_{(z,y)\in\Gamma_R} - ik_z^{(n)}\tilde{E}_n(z,y)|_{(z,y)\in\Gamma_R} = 0 \tag{48}$$

A key aspect of simplifying Eq. 36 is to substitute the basis expansion for $G(z,z_0,y,y_0) = \sum_{m=1}^{M_{total}} G_m(z,y,z_0,y_0)$ and $\tilde{E}(z,y)|_{(z,y)\in\Gamma_{L/R}} = \sum_{n=1}^{N_{total}} \tilde{E}_n(z,y)|_{(z,y)\in\Gamma_{L/R}}$ and their corresponding boundary conditions while simplifying.

$$\begin{aligned} \int \left\{ \textstyle\sum_n \tilde{E}_n(z,y) \frac{\partial}{\partial z} \sum_m G_m(z,y,z_0,y_0)\,\hat{e}_z - \sum_m G_m(z,y,z_0,y_0)\,\frac{\partial}{\partial z}\sum_n \tilde{E}_n(z,y)\hat{e}_z \right\}|_{(z,y)\in\Gamma_L} \cdot (-\hat{e}_z)\,dy + \\ \int \left\{ \textstyle\sum_n \tilde{E}_n(z,y) \frac{\partial}{\partial z} \sum_m G_m(z,y,z_0,y_0)\,\hat{e}_z - \sum_m G_m(z,y,z_0,y_0)\,\frac{\partial}{\partial z}\sum_n \tilde{E}_n(z,y)\hat{e}_z \right\}|_{(z,y)\in\Gamma_R} \cdot \hat{e}_z dy \\ = \tilde{E}(z_0,y_0)\,|_{(z_0,y_0)\in\Omega} \end{aligned} \tag{49}$$

As there is a $\chi_m(y)$ in $G_m(z,y,z_0,y_0)$ and a $\chi_n(y)$ in $\tilde{E}_n(z,y)$, due to orthogonality relation that $\int \chi_m(y)\chi_n(y)dy = \delta_{kron}(m,n)$, y integral of all the cross product terms where $m \neq n$, is zero. Hence only the terms $m = n$ remains non-zero. Therefore,

$$\begin{aligned} \int \textstyle\sum_n \left\{ \tilde{E}_n(z,y) \frac{\partial}{\partial z} G_n(z,y,z_0,y_0)\,\hat{e}_z - G_n(z,y,z_0,y_0)\,\frac{\partial}{\partial z}\tilde{E}_n(z,y)\hat{e}_z \right\}|_{(z,y)\in\Gamma_L} \cdot (-\hat{e}_z)\,dy + \\ \int \textstyle\sum_n \left\{ \tilde{E}_n(z,y) \frac{\partial}{\partial z} G_n(z,y,z_0,y_0)\,\hat{e}_z - G_n(z,y,z_0,y_0)\,\frac{\partial}{\partial z}\tilde{E}_n(z,y)\hat{e}_z \right\}|_{(z,y)\in\Gamma_R} \cdot \hat{e}_z dy = \tilde{E}(z_0,y_0)\,|_{(z_0,y_0)\in\Omega} \end{aligned} \tag{50}$$

Substituting the previously obtained boundary conditions (equations Eq. 35, Eq. 48, Eq. 34 and Eq. 43) in the above given form of boundary integral, the following simplified expression is obtained after some simple calculations.

$$\int \sum_n 2ik_z^{(n)} \tilde{E}_n^{inc}(z,y) G_n(z,y,z_0,y_0)\,|_{(z,y)\in\Gamma_L} dy = \tilde{E}(z_0,y_0)|_{(z_0,y_0)\in\Omega} \tag{51}$$

One could safely add a summation $\sum_m$ to the $G_m(z,y,z_0,y_0)$ term in the above equation due to the orthogonality relationship $\int \chi_m(y)\chi_n(y)dy = \delta_{kron}(m,n)$. Therefore, the meaning of the integral given in Eq. 51 doesn't change if it is written in the following form

$$\int \sum_n 2ik_z^{(n)} \tilde{E}_n^{inc}(z,y) \sum_m G_m(z,y,z_0,y_0)\,|_{(z,y)\in\Gamma_L} dy = \tilde{E}(z_0,y_0)|_{(z_0,y_0)\in\Omega} \tag{52}$$

Replacing the expression for $\sum_m G_m(z,y,z_0,y_0)$ as $G(z,y,z_0,y_0)$ and changing the index n to m, the boundary integral takes a simpler form as given below. For wave incidence only from the left to right of the disorder (incidence onto Γ_L),

$$\sum_{m=1}^{M_{total}} 2ik_z^{(m)} \int \tilde{E}_m^{inc}(z,y) G(z,y,z_0,y_0)\,|_{(z,y)\in\Gamma_L} dy = \tilde{E}(z_0,y_0)\,|_{(z_0,y_0)\in\Omega} \tag{53}$$

where $\tilde{E}_m^{inc}(z,y)|_{(z,y)\in\Gamma_L} = c_m^+\psi_m^+(z,y)|_{(z,y)\in\Gamma_L}$, $k_z^{(m)} = ik_{z,ev}^{(m)}$ when $m > M_{pr}$ and $M_{total} = M_{pr} + M_{ev}$, the total number of eigenmodes considered.

VI. DERIVATION OF GENERALIZED FISHER-LEE RELATIONSHIPS

Generalized Fisher-Lee relations are obtained by substituting expression for the total field $\tilde{E}(z_0, y_0)$ in the boundary integral equation and solving for the reflection or transmission coefficients.

A. Derivation for S_{21}

Let the wave incidence be from the left side of the disorder onto Γ_L. For estimating the transmission matrix S_{21}, need to take $(z_0, y_0) \in \Gamma_R$. Then the simplified boundary integral equation becomes,

$$\begin{aligned}\sum_{m=1}^{M_{total}} 2ik_z^{(m)} \int \tilde{E}_m^{inc}(z,y) G(z,y,z_0,y_0)\, dy|_{(z,y)\in\Gamma_L \& (z_0,y_0)\in\Gamma_R} &= \tilde{E}(z_0,y_0)|_{(z_0,y_0)\in\Gamma_R} = \sum_{n=1}^{N_{total}} \tilde{E}_n(z_0,y_0)\,|_{(z_0,y_0)\in\Gamma_R} \\ &= \sum_{n=1}^{N_{total}} t_n^+ \chi_n(y_0)\phi_n^+(z_0)|_{(z_0,y_0)\in\Gamma_R} \\ &= \sum_{n=1}^{N_{total}} \left\{ \sum_{m=1}^{M_{total}} c_m^+ S_{21}^{nm} \right\} \chi_n(y_0)\phi_n^+(z_0)|_{(z_0,y_0)\in\Gamma_R} \quad (54)\end{aligned}$$

Since this equation holds for any incident wave represented by any set of c_m^+ values, one can collect the terms multiplied by c_m^+ and spanned by $\sum_{m=1}^{M_{total}}$ on both the L.H.S and R.H.S, and solve for $\mathbf{S}_{21}^{nm}$.

$$2ik_z^{(m)} \int \phi_m^+(z)\chi_m(y) G(z,y,z_0,y_0)\, dy|_{(z,y)\in\Gamma_L \& (z_0,y_0)\in\Gamma_R} = \sum_{n=1}^{N_{total}} S_{21}^{nm} \chi_n(y_0)\phi_n^+(z_0)|_{(z_0,y_0)\in\Gamma_R} \quad (55)$$

Using the orthogonality relationship involving $\chi_{n'}(y)$ and integrating with respect to y_0 on both sides of the above given equation,

$$2ik_z^{(m)}\phi_m^+(z) \int_y \int_{y_0} \chi_m(y) G(z,y,z_0,y_0)\, \chi_{n'}(y_0) dy dy_0|_{(z,y)\in\Gamma_L \& (z_0,y_0)\in\Gamma_R} = S_{21}^{n'm}\phi_{n'}^+(z_0)|_{z_0\in\Gamma_R} \quad (56)$$

Simplification : Rename n' as n and let z be positioned at 0 on the left boundary and $z_0 = z_R$ at Γ_R on the right boundary. Therefore,

$$\begin{aligned}&2ik_z^{(m)}\phi_m^+(z=0) \int_y \int_{y_0} \chi_m(y) G(z=0,y,z_0=z_R,y_0)\, \chi_n(y_0) dy dy_0|_{(z=0,y)\in\Gamma_L \& (z_0=z_R,y_0)\in\Gamma_R} = \\ &S_{21}^{nm}\phi_n^+(z_0=z_R)|_{(z_0=z_R)\in\Gamma_R} \quad (57)\end{aligned}$$

Mathematically, there are 4 different possibilities with respect to the nature of incident and transmitted modes.
Case 1 : Both input and output modes are propagating $m \le M_{prop}$ and $n \le N_{prop}$

$$2ik_z^{(m)} \frac{1}{\sqrt{k_z^{(m)}}} \int_y \int_{y_0} \chi_m(y) G(z,y,z_0,y_0)\, \chi_n(y_0) dy dy_0|_{(z=0,y)\in\Gamma_L \& (z_0=z_R,y_0)\in\Gamma_R} = S_{21}^{nm} \frac{1}{\sqrt{k_z^{(n)}}} e^{+ik_z^{(n)} z_R} \quad (58)$$

Case 2 : Input mode and output modes are evanescent $m > M_{prop}$ and $n > N_{prop}$

$$2ik_z^{(m)} \frac{1}{\sqrt{\left|k_z^{(m)}\right|}} \int_y \int_{y_0} \chi_m(y) G(z,y,z_0,y_0)\, \chi_n(y_0) dy dy_0|_{(z,y)\in\Gamma_L \& (z_0,y_0)\in\Gamma_R} = S_{21}^{nm} \frac{1}{\sqrt{\left|k_z^{(n)}\right|}} \quad (59)$$

Case 3 : Input modes are propagating and output modes are evanescent $m \le M_{prop}$ and $n > N_{prop}$

$$2ik_z^{(m)} \frac{1}{\sqrt{k_z^{(m)}}} \int_y \int_{y_0} \chi_m(y) G(z,y,z_0,y_0)\, \chi_n(y_0) dy dy_0|_{(z,y)\in\Gamma_L \& (z_0,y_0)\in\Gamma_R} = S_{21}^{nm} \frac{1}{\sqrt{\left|k_z^{(n)}\right|}} \quad (60)$$

Case 4 : Input modes are evanescent and output modes are propagating $m > M_{prop}$ and $n \leq N_{prop}$

$$2ik_z^{(m)} \frac{1}{\sqrt{\left|k_z^{(m)}\right|}} \int_y \int_{y_0} \chi_m(y) G\left(z, y, z_0, y_0\right) \chi_n(y_0) dy dy_0|_{(z,y)\in\Gamma_L \& (z_0,y_0)\in\Gamma_R} = S_{21}^{nm} \frac{e^{+iz_R k_z^{(n)}}}{\sqrt{k_z^{(n)}}} \tag{61}$$

Solving for S_{21} for cases $1, 2, 3$ and 4 (using the information that for evanescent modes $\frac{k_z^{(m)}}{\sqrt{|k_z^{(m)}|}} = i\sqrt{|k_z^{(m)}|}$, is imaginary) are summarised in the Table III.

B. Derivation for S_{22}

Let the wave incidence be from the right side of the disorder onto Γ_R. For estimating the reflection matrix S_{22}, need to take $(z_0, y_0) \in \Gamma_R$. Then the simplified boundary integral equation becomes,

$$\begin{aligned}
&\sum_{m=1}^{M_{total}} 2ik_z^{(m)} \int E_m^{\text{inc}}(z, y) G\left(z, y, z_0, y_0\right) dy|_{(z,y)\in\Gamma_R \& (z_0,y_0)\in\Gamma_R} = \sum_{n=1}^{N_{total}} \tilde{E}_n\left(z_0, y_0\right)|_{(z_0,y_0)\in\Gamma_R} \\
&= \sum_{m=1}^{M_{total}} \sum_{n=1}^{N_{total}} c_m^- \left[\delta_{\text{kron}}(n, m) \phi_n^-(z_0) \chi_n(y_0) + S_{22}^{nm} \chi_n(y_0) \phi_n^+(z_0)\right]|_{(z_0,y_0)\in\Gamma_R}
\end{aligned} \tag{62}$$

Performing the same set of operations as used for the derivation of S_{11} and setting $z = z_R$ and $z_0 = z_R$, the following is obtained

$$\begin{aligned}
&2ik_z^{(m)} \phi_m^-(z = z_R) \int_{y_0} \int_y \chi_m(y) G\left(z = z_R, y, z_0 = z_R, y_0\right) \chi_n(y_0)|_{(z=z_R,y)\in\Gamma_R \& (z_0=z_R,y_0)\in\Gamma_R} dy dy_0 = \\
&\left\{\delta_{\text{kron}}(n, m) \phi_n^-(z_0 = z_R) + S_{22}^{nm} \phi_n^+(z_0 = z_R)\right\}|_{z_0=z_R\in\Gamma_R}
\end{aligned} \tag{63}$$

Mathematically, there are 4 different possibilities with respect to the nature of incident and reflected modes.

Case 1 : Both input and output modes are propagating $m \leq M_{prop}$ and $n \leq N_{prop}$

$$\begin{aligned}
&2ik_z^{(m)} \frac{e^{-iz_R k_z^{(m)}}}{\sqrt{k_z^{(m)}}} \int_{y_0} \int_y \chi_m(y) G\left(z, y, z_0, y_0\right) \chi_n(y_0)|_{(z=z_R,y)\in\Gamma_R \& (z_0=z_R,y_0)\in\Gamma_R} dy dy_0 = \\
&\delta_{\text{kron}}(n, m) \frac{e^{-iz_R k_z^{(n)}}}{\sqrt{k_z^{(n)}}} + S_{22}^{nm} \frac{e^{+iz_R k_z^{(n)}}}{\sqrt{k_z^{(n)}}}
\end{aligned} \tag{64}$$

Case 2 : Input mode and output modes are evanescent $m > M_{prop}$ and $n > N_{prop}$

$$\begin{aligned}
&2ik_z^{(m)} \frac{1}{\sqrt{\left|k_z^{(m)}\right|}} \int_{y_0} \int_y \chi_m(y) G\left(z, y, z_0, y_0\right) \chi_n(y_0)|_{(z=z_R,y)\in\Gamma_R \& (z_0=z_R,y_0)\in\Gamma_R} dy dy_0 = \\
&\delta_{\text{kron}}(n, m) \frac{1}{\sqrt{\left|k_z^{(n)}\right|}} + S_{22}^{nm} \frac{1}{\sqrt{\left|k_z^{(n)}\right|}}
\end{aligned} \tag{65}$$

Case 3 : Input modes are propagating and output modes are evanescent $m \leq M_{prop}$ and $n > N_{prop}$

$$2ik_z^{(m)}\frac{e^{-iz_Rk_z^{(m)}}}{\sqrt{k_z^{(m)}}}\int_{y_0}\int_y \chi_m(y)G\left(z,y,z_0,y_0\right)\chi_n(y_0)|_{(z,y)\in\Gamma_R\&(z_0,y_0)\in\Gamma_R}dydy_0 =$$
$$\delta_{\text{kron}}(n,m)\frac{e^{-iz_Rk_z^{(n)}}}{\sqrt{k_z^{(n)}}} + S_{22}^{nm}\frac{1}{\sqrt{\left|k_z^{(n)}\right|}} \tag{66}$$

But $\delta_{\text{kron}}(n,m)=0$, if $m\leq M_{\text{prop}}$ and $n>N_{\text{prop}}$.
Case 4 : Input modes are evanescent and output modes are propagating $m>M_{prop}$ and $n\leq N_{prop}$

$$2ik_z^{(m)}\frac{1}{\sqrt{\left|k_z^{(m)}\right|}}\int_{y_0}\int_y \chi_m(y)G\left(z,y,z_0,y_0\right)\chi_n(y_0)|_{(z,y)\in\Gamma_R\&(z_0,y_0)\in\Gamma_R}dydy_0 =$$
$$\delta_{\text{kron}}(n,m)\frac{1}{\sqrt{\left|k_z^{(n)}\right|}} + S_{22}^{nm}\frac{e^{+iz_Rk_z^{(n)}}}{\sqrt{k_z^{(n)}}} \tag{67}$$

But $\delta_{\text{kron}}(n,m)=0$, if $m>M_{\text{prop}}$ and $n\leq N_{\text{prop}}$.
Solving S_{22} for cases $1,2,3$ and 4 (using the information that for evanescent modes $\frac{k_z^{(m)}}{\sqrt{|k_z^{(m)}|}}=i\sqrt{|k_z^{(m)}|}$, is imaginary) are summarised in the Table IV.

C. Derivation for S_{12}

Let the wave incidence be from the right side of the disorder onto Γ_R. For estimating the transmission matrix S_{12}, need to take $(z_0,y_0)\in\Gamma_L$. Then the simplified boundary integral equation becomes,

$$\sum_{m=1}^{M_{total}} 2ik_z^{(m)}\int \tilde{E}_m^{inc}(z,y)G\left(z,y,z_0,y_0\right)dy|_{(z,y)\in\Gamma_R\&(z_0,y_0)\in\Gamma_L} = \sum_{n=1}^{N_{total}}\tilde{E}_n\left(z_0,y_0\right)|_{(z_0,y_0)\in\Gamma_L}$$
$$= \sum_{n=1}^{N_{total}}\left\{\sum_{m=1}^{M_{total}} c_m^+S_{12}^{nm}\right\}\chi_n(y_0)\phi_n^-(z_0)|_{(z_0,y_0)\in\Gamma_L} \tag{68}$$

Performing the same set of operations as used for the derivation of S_{21} and setting $z=z_R$ and $z_0=z_L$, the following is obtained

$$2ik_z^{(m)}\phi_m^-(z=z_R)\int_y\int_{y_0}\chi_m(y)G\left(z=z_R,y,z_0=z_L,y_0\right)\chi_n(y_0)dydy_0|_{(z=z_R,y)\in\Gamma_R\&(z_0=z_L,y_0)\in\Gamma_L} =$$
$$S_{12}^{nm}\phi_{n'}^-(z_0)|_{(z_0=z_L)\in\Gamma_L} \tag{69}$$

Mathematically, there are 4 different possibilities with respect to the nature of incident and transmitted modes.

Case 1 : Both input and output modes are propagating $m\leq M_{prop}$ and $n\leq N_{prop}$

$$2ik_z^{(m)}\frac{e^{-iz_Rk_z^{(m)}}}{\sqrt{k_z^{(m)}}}\int_y\int_{y_0}\chi_m(y)G\left(z,y,z_0,y_0\right)\chi_n(y_0)dydy_0|_{(z=z_R,y)\in\Gamma_R\&(z_0=z_L,y_0)\in\Gamma_L} = S_{12}^{nm}\frac{1}{\sqrt{k_z^{(n)}}} \tag{70}$$

Case 2 : Input mode and output modes are evanescent $m>M_{prop}$ and $n>N_{prop}$

$$2ik_z^{(m)}\frac{1}{\sqrt{\left|k_z^{(m)}\right|}}\int_y\int_{y_0}\chi_m(y)G\left(z,y,z_0,y_0\right)\chi_n(y_0)dydy_0|_{(z=z_R,y)\in\Gamma_R\&(z_0=z_L,y_0)\in\Gamma_L} = S_{12}^{nm}\frac{1}{\sqrt{\left|k_z^{(n)}\right|}} \tag{71}$$

Case 3 : Input modes are propagating and output modes are evanescent $m \leq M_{prop}$ and $n > N_{prop}$

$$2ik_z^{(m)} \frac{e^{-iz_R k_z^{(m)}}}{\sqrt{k_z^{(m)}}} \int_y \int_{y_0} \chi_m(y) G\left(z, y, z_0, y_0\right) \chi_n(y_0) dy dy_0|_{(z=z_R, y)\in\Gamma_R \& (z_0=z_L, y_0)\in\Gamma_L} = S_{12}^{nm} \frac{1}{\sqrt{\left|k_z^{(n)}\right|}} \tag{72}$$

Case 4 : Input modes are evanescent and output modes are propagating $m > M_{prop}$ and $n \leq N_{prop}$

$$2ik_z^{(m)} \frac{1}{\sqrt{\left|k_z^{(m)}\right|}} \int_y \int_{y_0} \chi_m(y) G\left(z, y, z_0, y_0\right) \chi_n(y_0) dy dy_0|_{(z,y)\in\Gamma_L \& (z_0,y_0)\in\Gamma_R} = \frac{S_{12}^{nm}}{\sqrt{k_z^{(n)}}} \tag{73}$$

Solving S_{12} for cases $1, 2, 3$ and 4 (using the information that for evanescent modes $\frac{k_z^{(m)}}{\sqrt{|k_z^{(m)}|}} = i\sqrt{|k_z^{(m)}|}$, is imaginary) are summarized in the Table V.

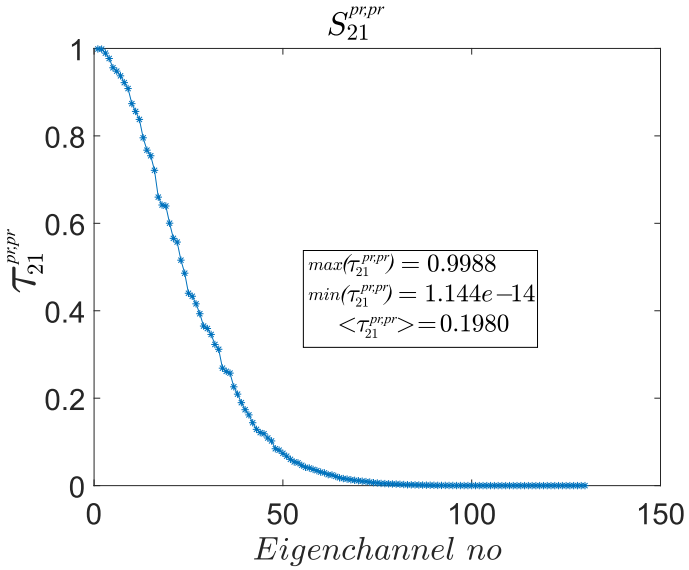


FIG. 1. **Eigenchannel transmission coefficients of $S_{21}^{pr,pr}$ are plotted for a disorder with the average eigenchannel transmission of 0.198**. Eigenchannel transmission coefficients contained in the diagonal of the matrix $\tau_{21}^{pr,pr}$, (obtained from the *S.V.D* of the $S_{21}^{pr,pr}$ matrix given in FIG. 2 of the main paper), is plotted. The maximum, minimum and average values of $\tau_{21}^{pr,pr}$ are also given. The averaging is done with respect to all the eigenchannels of the given disorder. Some of the corresponding eigenchannels are plotted in the supplementary FIG. 2.

VII. VISUALIZATION OF TRANSMISSION EIGENCHANNELS

For accessing the propagating eigenchannels, singular value decomposition (*S.V.D*) of the components of the $S^{pr,pr}$ matrix is performed. As an example, the propagating transmission eigenchannels for wave incidence only from the left-side of the disorder, is accessed by performing the *S.V.D* of $S_{21}^{pr,pr} = U_{21}\Sigma_{21}V_{21}^{\dagger}$ and using the first singular vector of V_{21} to maximize the transmission. $\tau_{21}^{pr,pr} = (\Sigma_{21}^{pr,pr})^2$ is the diagonal matrix containing the eigenchannels' transmission coefficients ranging from 0 to 1 as shown in the supplementary FIG. 1. For the disordered slab shown in FIG. 2(b) of the main paper, various eigenchannels, for the wave incidence from both the left side and the right side of the disorder, are shown in the supplementary FIG. 2.

VIII. ADDITIONAL NUMERICAL VALIDATION OF THE GENERALIZED UNITARITY RELATION

In addition to the numerical validation of the compact form of the generalized unitary relation given in the FIG. 8(a) of the main paper, additional validation is performed by decomposing the compact form into some of its individual components as given in the supplementary FIG. 3.

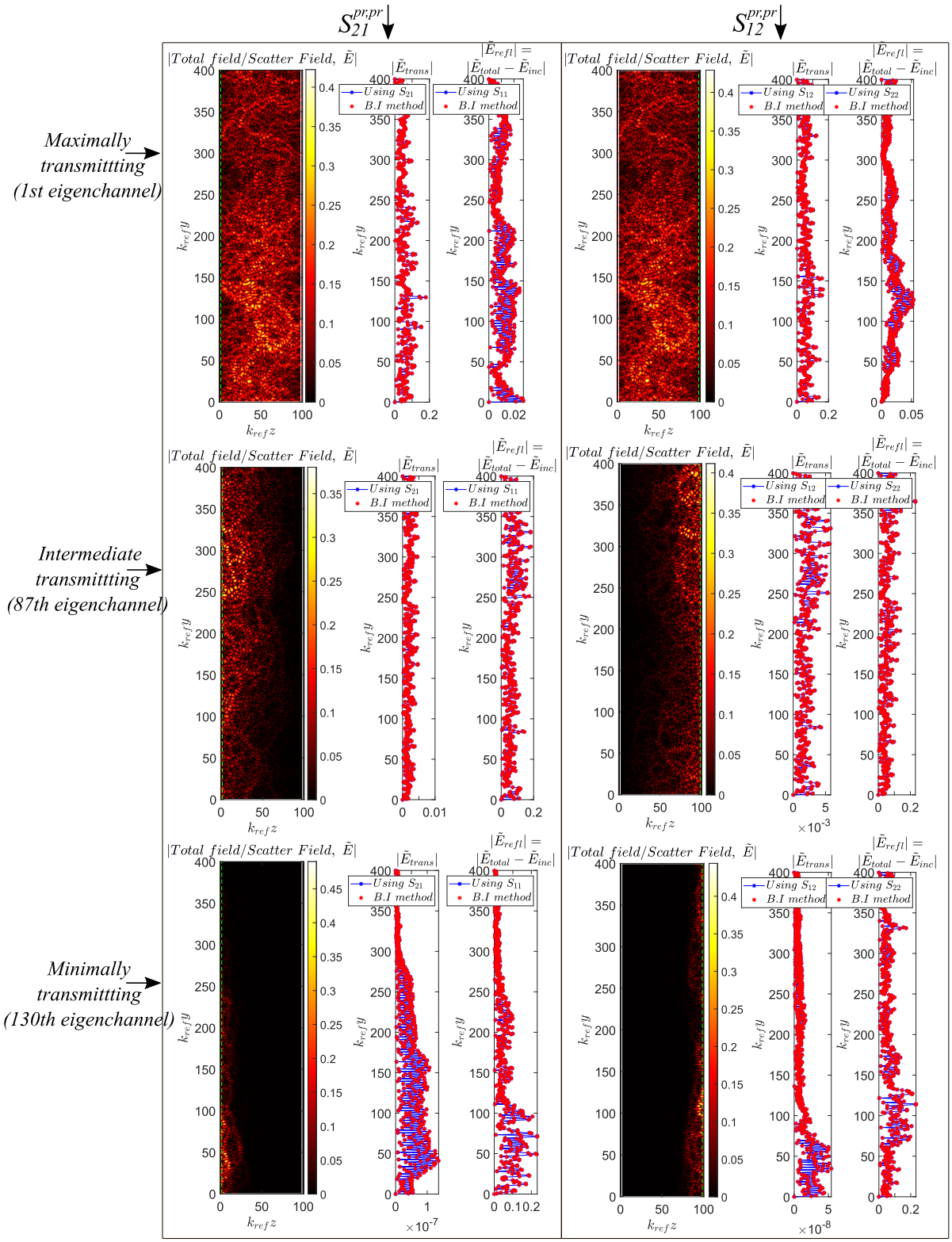


FIG. 2. **Visualizing various eigenchannels of $S_{21}^{pr,pr}$ and $S_{12}^{pr,pr}$, containing 130 propagating eigenmodes and 30 evanescent eigenmodes, with $\langle \tau_{21}^{pr,pr} \rangle = 0.198$, the transmission averaged over various eigenchannels of the given disorder shown in FIG. 2(b) of the main paper. (a)** Maximally transmitted (first) eigenchannel of $S_{21}^{pr,pr}$, where transmission, $T = 0.9988$ and reflection $R = 0.0012$ **(b)** An intermediate eigenchannel numbered 87 out of the 130 eigenchannel modes, of $S_{21}^{pr,pr}$, where $T = 0.0013, R = 0.9987$. **(c)** Minimally transmitted (last eigenchannel numbered 130) eigenchannel of $S_{21}^{pr,pr}$, where $T = 1.1438e-14, R = 1$. Similarly, **(d)** Maximally transmitted (first) eigenchannel of $S_{12}^{pr,pr}$, where $T = 0.9988, R = 0.0012$ **(e)** An intermediate eigenchannel numbered 87 out of the 130 eigenchannel modes, of $S_{12}^{pr,pr}$, where $T = 0.0013, R = 0.9987$. **(f)** Minimally transmitted (last eigenchannel, numbered 130) eigenchannel of $S_{12}^{pr,pr}$, where $T = 1.1438e-14, R = 1$. The transport paths associated with the maximally transmitted eigenchannel of $S_{21}^{pr,pr}$ and $S_{12}^{pr,pr}$ looks identical in the inside of the disorder. It is because the transport path taken from left to right with the maximum transmission close to unity, is the same path taken from right to left for maximal transmission.

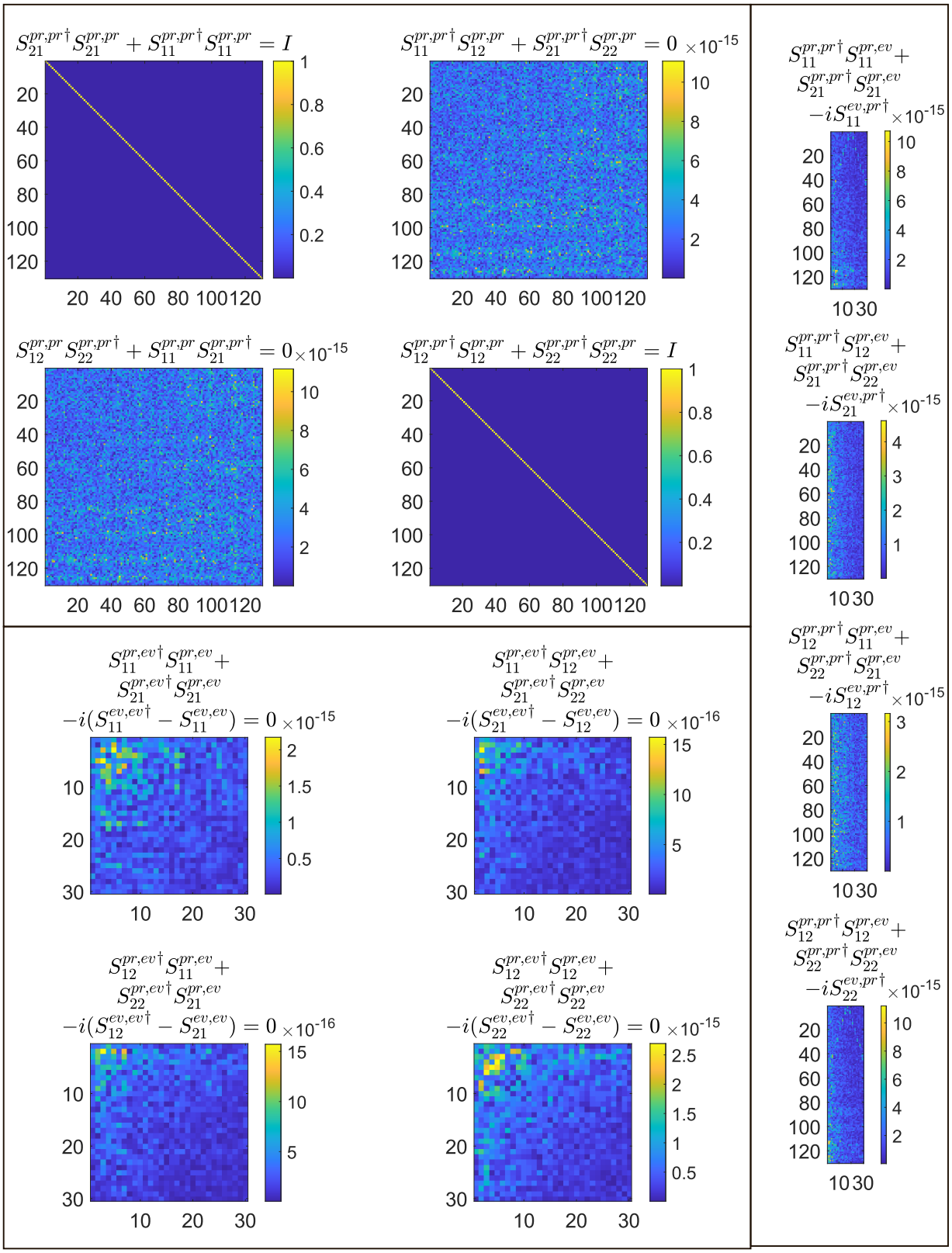


FIG. 3. **Additional numerical validation done for verifying the generalized unitarity relations**. For those unitarity relations where the R.H.S is a zero matrix analytically, the simulation code yields a numerical matrix close to be approximated to zero (of the order of 10^{-15}) as shown in the plots. For those unitarity relations where the R.H.S is a unit matrix analytically, the diagonal elements are all unity.

IX. S MATRIX CASCADING AND ENSEMBLE AVERAGING

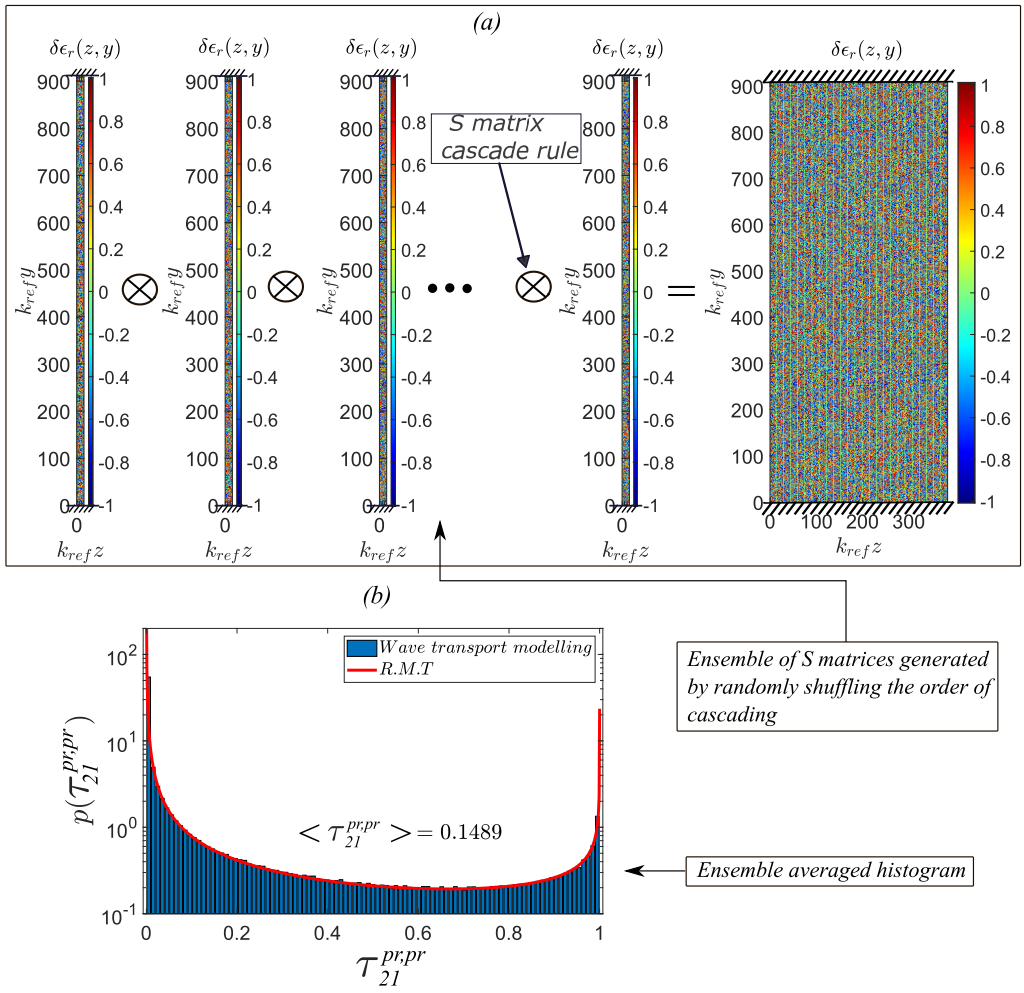


FIG. 4. **Schematic to demonstrate the S matrix cascade rule and the ensemble averaged eigenchannel transmission coefficient distribution obtained through cascading. (a)** Schematic of cascading thinner slabs to form thicker slab is shown. Cascade rule given in Eq. 76 is used to cascade the slabs. First, the first and the second thin slabs are cascaded. It is followed by cascading the third slab with the cascaded result obtained from the first and the second slab. This pattern is repeated, until the last thin slab is cascaded. **(b)** The ensemble averaged frequency distribution of $\tau_{21}^{pr,pr}$ values after cascading. It is compared with the bimodal distribution associated with the Random Matrix theory ($R.M.T$). Note that here the histogram is evaluated for individual cascaded disorders, followed by averaging the obtained histogram over many cascaded disorder realizations.

This section explains the S matrix cascading method by which, a larger disordered slab can be formed, by cascading an ensemble of thinner slabs. Cascading of the generalized S matrices of the thinner slabs, builds the sample along the longitudinal dimension (z axis) step-by-step, as shown in the schematic given in the supplementary FIG. 4(a). Different realizations of thicker slabs (1000 in number) can be formed from the same S matrices of the thinner slabs (25 in number), taken in random order. This is particularly advantageous from a computational point of view that, one need not model 1000 different large slabs, but could estimate the S matrices of a collection of smaller slabs once and cascade them using random order of the slabs for obtaining different realizations of larger slabs. The well known cascading formula for S matrices is given as the following.

$$S^{(a)} = \begin{pmatrix} S_{11}^{(a)} & S_{12}^{(a)} \\ S_{21}^{(a)} & S_{22}^{(a)} \end{pmatrix} \tag{74}$$

and

$$S^{(b)} = \begin{pmatrix} S_{11}^{(b)} & S_{12}^{(b)} \\ S_{21}^{(b)} & S_{22}^{(b)} \end{pmatrix} \tag{75}$$

$$\begin{aligned} S^{\text{cascade}} &= S^{(a)} \bigotimes S^{(b)} = \begin{pmatrix} S_{11}^{(a)} & S_{12}^{(a)} \\ S_{21}^{(a)} & S_{22}^{(a)} \end{pmatrix} \bigotimes \begin{pmatrix} S_{11}^{(b)} & S_{12}^{(b)} \\ S_{21}^{(b)} & S_{22}^{(b)} \end{pmatrix} \\ &= \begin{pmatrix} S_{11}^{(a)} + S_{12}^{(a)} \left(I - S_{11}^{(b)} S_{22}^{(a)}\right)^{-1} S_{11}^{(b)} S_{21}^{(a)} & S_{12}^{(a)} \left(I - S_{11}^{(b)} S_{22}^{(a)}\right)^{-1} S_{12}^{(b)} \\ S_{21}^{(b)} \left(I - S_{22}^{(a)} S_{11}^{(b)}\right)^{-1} S_{21}^{(a)} & S_{22}^{(b)} + S_{21}^{(b)} \left(I - S_{22}^{(a)} S_{11}^{(b)}\right)^{-1} S_{22}^{(a)} S_{12}^{(b)} \end{pmatrix} \end{aligned} \tag{76}$$

where I is the identity matrix. The S matrices for a collection of the smaller slabs, are estimated serially using the generalized Fisher-Lee relations, followed by the use of the cascading formula given in Eq. 76. This helps in the ensemble averaging of the focusing results in the main paper. The ensemble averaged eigenchannel transmission coefficients of $S_{21}^{pr,pr}$ after cascading is given in FIG. 4(b).